

# Matching the Decay Half-Life with the Biological Half-Life: ImmunoPET Imaging with $^{44}\text{Sc}$ -Labeled Cetuximab Fab Fragment

Rubel Chakravarty,<sup>#,†,‡</sup> Shreya Goel,<sup>#,§</sup> Hector F. Valdovinos,<sup>||</sup> Reinier Hernandez,<sup>||</sup> Hao Hong,<sup>†</sup> Robert J. Nickles,<sup>||</sup> and Weibo Cai<sup>\*,†,||,⊥</sup>

<sup>†</sup>Department of Radiology, University of Wisconsin–Madison, Madison, Wisconsin 53792, United States

<sup>‡</sup>Isotope Production and Applications Division, Bhabha Atomic Research Centre, Mumbai 400085, India

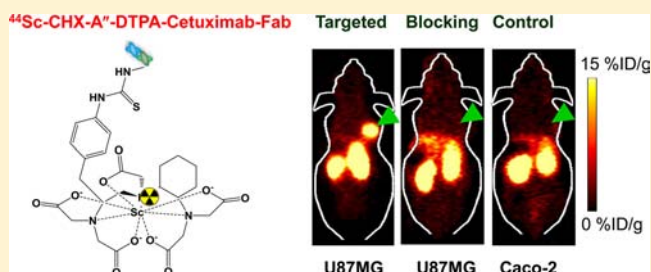
<sup>§</sup>Materials Science Program, University of Wisconsin–Madison, Madison, Wisconsin 53706, United States

<sup>||</sup>Department of Medical Physics, University of Wisconsin–Madison, Madison, Wisconsin 53705, United States

<sup>⊥</sup>University of Wisconsin Carbone Cancer Center, Madison, Wisconsin 53792, United States

## S Supporting Information

**ABSTRACT:** Scandium-44 ( $t_{1/2} = 3.9$  h) is a relatively new radioisotope of potential interest for use in clinical positron emission tomography (PET). Herein, we report, for the first time, the room-temperature radiolabeling of proteins with  $^{44}\text{Sc}$  for *in vivo* PET imaging. For this purpose, the Fab fragment of Cetuximab, a monoclonal antibody that binds with high affinity to epidermal growth factor receptor (EGFR), was generated and conjugated with *N*-[(*R*)-2-amino-3-(*para*-isothiocyanato-phenyl)propyl]-*trans*-(*S,S*)-cyclohexane-1,2-diamine-*N,N,N',N''*,*N''*-pentaacetic acid (CHX-A''-DTPA). The high purity of Cetuximab-Fab was confirmed by SDS-PAGE and mass spectrometry. The potential of the bioconjugate for PET imaging of EGFR expression in human glioblastoma (U87MG) tumor-bearing mice was investigated after  $^{44}\text{Sc}$  labeling. PET imaging revealed rapid tumor uptake (maximum uptake of  $\sim 12\%$  ID/g at 4 h postinjection) of  $^{44}\text{Sc}$ -CHX-A''-DTPA-Cetuximab-Fab with excellent tumor-to-background ratio, which might allow for same day PET imaging in future clinical studies. Immunofluorescence staining was conducted to correlate tracer uptake in the tumor and normal tissues with EGFR expression. This successful strategy for immunoPET imaging of EGFR expression using  $^{44}\text{Sc}$ -CHX-A''-DTPA-Cetuximab-Fab can make clinically translatable advances to select the right population of patients for EGFR-targeted therapy and also to monitor the therapeutic efficacy of anti-EGFR treatments.



## INTRODUCTION

Scandium-44 is a relatively new radioisotope with excellent nuclear decay characteristics [ $t_{1/2} = 3.9$  h,  $E_{\beta^+}$  (max) = 1.47 MeV,  $\beta^+$  branching ratio = 94.3%] for PET imaging.<sup>1</sup> The radioisotope can be conveniently produced in a cyclotron by irradiation of Ca targets with protons by the nuclear reaction  $^{44}\text{Ca}(p,n)^{44}\text{Sc}$ .<sup>2,3</sup> The longer half-life of  $^{44}\text{Sc}$  compared to that of other more commonly used PET radioisotopes such as  $^{18}\text{F}$  ( $t_{1/2} = 109$  min) or  $^{68}\text{Ga}$  ( $t_{1/2} = 68$  min) potentially allows for the centralized production and cost-efficient distribution of  $^{44}\text{Sc}$ -based radiopharmaceuticals regionally. Another advantage lies in the availability of  $^{47}\text{Sc}$  ( $t_{1/2} = 3.35$  days), which is a moderate energy (0.6 MeV, 100%)  $\beta^-$  emitter suitable for targeted therapy.<sup>3</sup> By coupling to the same biological vector,  $^{44}\text{Sc}$  can be used as an imaging surrogate for  $^{47}\text{Sc}$  and might also aid in estimating dosimetry for therapy with  $^{47}\text{Sc}$ , thereby representing an ideal theranostic pair.

Despite these excellent attributes, only limited number of  $^{44}\text{Sc}$  radiopharmaceuticals based on peptides and other small biomolecules has been reported to date.<sup>4–7</sup> In all of these

studies, 1,4,7,10-tetraazacyclododecane-1,4,7,10-tetraacetic acid (DOTA) was used as the bifunctional chelator (BFC), and radiolabeling was carried out at  $\sim 95$  °C. Although  $^{44}\text{Sc}$ -DOTA complexes are formed with high *in vivo* stability,<sup>1,8</sup> the relatively slow complexation kinetics and requirement of elevated temperature for complex formation impede the preparation of radiotracers comprising temperature-sensitive and fragile macromolecules such as proteins. In view of this, it is essential to identify a suitable BFC that can be radiolabeled with  $^{44}\text{Sc}$  at room temperature within a reasonable period of time and that also demonstrates high *in vitro* and *in vivo* stability. The feasibility to radiolabel  $^{44}\text{Sc}$  with proteins such as antibody fragments would enhance the scope of  $^{44}\text{Sc}$ -radiopharmacy and facilitate utilization of this radioisotope for immunoPET imaging.

Over the last few decades, EGFR has been investigated as a major target for uncontrolled tumor growth in various types of

**Received:** September 4, 2014

**Revised:** November 10, 2014

**Published:** November 11, 2014

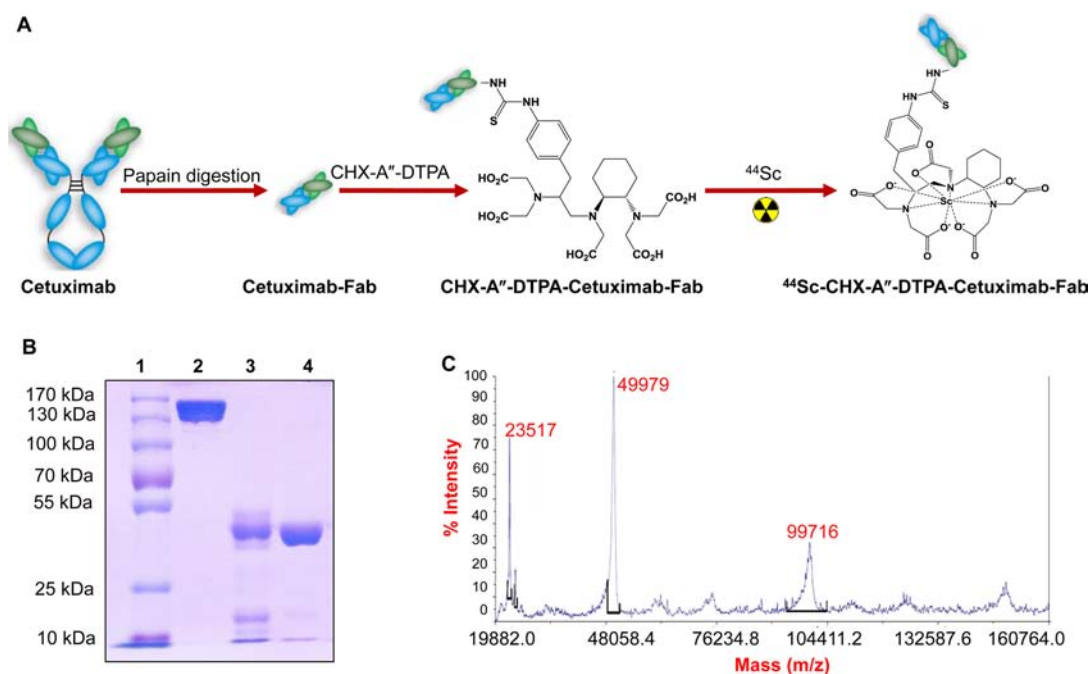


**Figure 1.** Generation of Cetuximab-Fab and its characterization. (A) Schematic diagram for Cetuximab-Fab generation from intact antibody, conjugation, and radiolabeling. The figures are not drawn to scale. (B) SDS-PAGE to confirm the purity of Cetuximab-Fab (lane 1, ladder; lane 2, intact Cetuximab; lane 3, unpurified Cetuximab-Fab after papain digestion; and lane 4, purified Cetuximab-Fab after passing through Protein A column). (C) Mass spectrometry of Cetuximab-Fab (~49.9 kDa).

cancers.<sup>9</sup> Cetuximab is a chimeric human–murine IgG1 monoclonal antibody that binds specifically to EGFR with high affinity.<sup>10,11</sup> Delayed tumor uptake and prolonged circulation half-life are the major limitations toward the use of intact antibodies as molecular imaging probes.<sup>12–14</sup> In order to accelerate targeting of EGFR, Cetuximab-F(ab')<sub>2</sub> fragments were earlier generated and radiolabeled with <sup>111</sup>In.<sup>15,16</sup> However, it took several hours to obtain satisfactory contrast between the tumor and normal tissues after administration of the radiolabeled agent.<sup>16</sup> This is especially disadvantageous when repeated imaging is required within short time intervals, for example, when studying the dynamics of EGFR expression during treatment. Therefore, we aimed to further improve EGFR targeting kinetics by using monovalent (Fab) fragments of Cetuximab for PET imaging. Cetuximab-Fab fragments, comprising both V<sub>H</sub> and V<sub>L</sub> domains, are expected to retain the specificity and antigen-binding affinity of the parent antibody while demonstrating improved pharmacokinetics for tissue penetration.<sup>12</sup> The decay half-life of <sup>44</sup>Sc matches the biological half-life of Fab fragments, which is another desirable feature for successful immunoPET imaging.<sup>12</sup>

Herein, we report the generation of a Cetuximab-Fab fragment and its radiolabeling with <sup>44</sup>Sc at room temperature using CHX-A''-DTPA (N-[(R)-2-amino-3-(para-isothiocyanato-phenyl) propyl]-trans-(S,S)-cyclohexane-1,2-diamine-N,N,N',N'',N''-pentaacetic acid) as the BFC. The *in vitro* and *in vivo* characteristics of <sup>44</sup>Sc-CHX-A''-DTPA-Cetuximab-Fab were investigated for PET imaging of EGFR expression in a human glioblastoma (U87MG) tumor model. The present study is the first report, to the best of our knowledge, of the radiolabeling and preclinical evaluation of <sup>44</sup>Sc-labeled protein molecules. This strategy can be extended for radiolabeling other temperature-sensitive biomolecules with <sup>44</sup>Sc for PET imaging.

## RESULTS

**Generation of Cetuximab-Fab and Its Characterization.** Cetuximab-Fab was generated from the intact antibody upon papain digestion for 4 h (Figure 1A). Protein A columns were used for separation of Cetuximab-Fab from the intact antibody and Fc fragments. The Protein A resin binds specifically to the Fc region of immunoglobulin molecules, especially IgGs,<sup>17–19</sup> allowing intact antibody and the Fc fragments generated during papain digestion to be trapped in the column and purified Cetuximab-Fab to pass through. Purified Cetuximab-Fab solution was further concentrated and buffer exchanged into PBS by ultrafiltration. SDS-PAGE showed the disappearance of the intact Cetuximab band (~150 kDa) and the appearance of a band corresponding to Cetuximab-Fab (~50 kDa), indicating complete digestion of Cetuximab by papain to yield a high-quality Fab fragment (Figure 1B). The molecular weight of Cetuximab-Fab, as determined by mass spectrometry, was ~49.9 kDa (Figure 1C). The purified Cetuximab-Fab was further used for bioconjugation and preclinical investigation in targeted, blocking, and negative control groups. For non-targeted groups, the purified Fab fragments were denatured by high-energy ultrasonication for over 1 h.

**Flow Cytometry.** To confirm that the generated Cetuximab-Fab retained the EGFR-binding characteristics of the intact antibody, *in vitro* targeting experiments were carried out using U87MG (high EGFR expression) and Caco-2 (low EGFR expression) cells for flow cytometry. Fluorescein isothiocyanate (FITC; excitation = 494 nm/emission = 521 nm) conjugated Cetuximab-Fab (50 nM) significantly enhanced the mean fluorescence intensity of U87MG cells (~20-fold higher than that of unstained cells), whereas treatment with a blocking dose of Cetuximab (1 μM) reduced the cell fluorescence by about 10-fold (Figure 2A). These

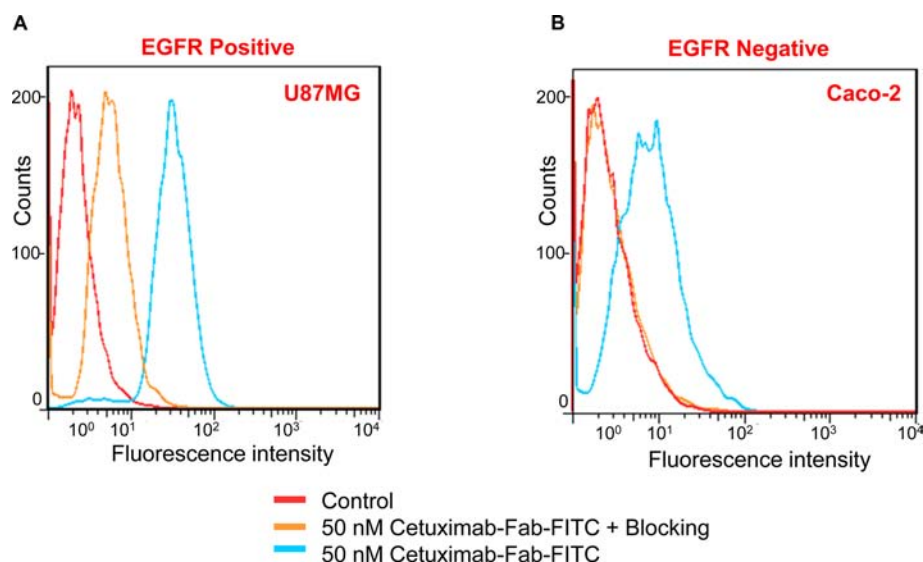


**Figure 2.** Flow cytometry in U87MG (high EGFR expression) and Caco-2 (low EGFR expression) cells confirms the EGFR specificity and affinity of Cetuximab-Fab.

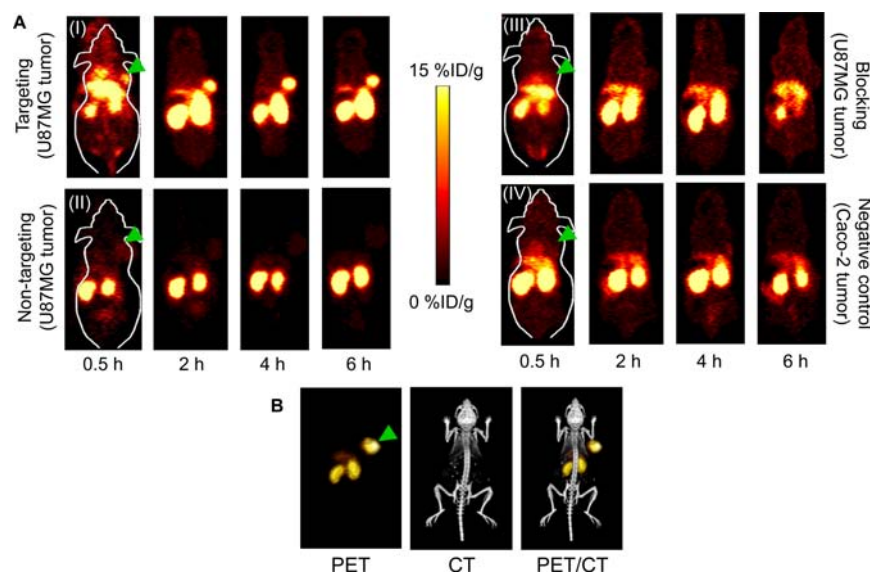


**Figure 3.** Serial PET imaging of EGFR expression. (A) Serial coronal PET images at 0.5, 2, 4, and 6 h p.i. of (I)  $^{44}\text{Sc}$ -CHX-A''-DTPA-Cetuximab-Fab in U87MG tumor-bearing mice (targeted), (II)  $^{44}\text{Sc}$ -CHX-A''-DTPA-denatured-Cetuximab-Fab in U87MG tumor-bearing mice (non-targeted), (III)  $^{44}\text{Sc}$ -CHX-A''-DTPA-Cetuximab-Fab after treatment with a 2 mg blocking dose of Cetuximab before injection in U87MG tumor-bearing mice, and (IV)  $^{44}\text{Sc}$ -CHX-A''-DTPA-Cetuximab-Fab in Caco-2 tumor-bearing mice (negative control). (B) Representative PET/CT images of U87MG tumor-bearing mouse at 4 h p.i. of  $^{44}\text{Sc}$ -CHX-A''-DTPA-Cetuximab-Fab. Arrowheads indicate tumors.

results demonstrate that FITC-Cetuximab-Fab specifically binds to EGFR on the U87MG cells. Meanwhile, the fluorescence signal from Caco-2 cells was minimal, indicating low nonspecific binding of FITC-Cetuximab-Fab (Figure 2B). The differences in the mean fluorescence intensities of U87MG and Caco-2 cells for targeted and blocking groups are shown in Figure S1. The control groups for both cell types show similar fluorescence background, which confirms that FITC-Cetuximab-Fab exhibits strong and specific binding to EGFR with negligible nonspecific binding *in vitro*. Papain digestion, therefore, does not compromise the EGFR-binding specificity of Cetuximab-Fab, thereby encouraging further *in vivo* studies.

**$^{44}\text{Sc}$  Labeling of Cetuximab-Fab and Serum Stability Evaluation.** Both intact and denatured Cetuximab-Fab fragments were labeled with  $^{44}\text{Sc}$  for *in vivo* studies (see

Experimental Section). The labeling conditions were carefully optimized to give the highest radiolabeling yields (see Supporting Information, experimental section and Figure S2). The radiolabeled bioconjugates were purified using PD-10 columns with PBS as the mobile phase. The radioactive fractions, which typically elute between 3 and 4 mL, were collected for further experiments, and a typical size-exclusion column chromatography profile can be seen in Figure S3A. The unreacted  $^{44}\text{Sc}$  starts eluting from the column after 6.0 mL. The decay-corrected radiochemical yields of Cetuximab-Fab conjugated with different BFCs are summarized in Table S1. Only DTPA analogues were found to be suitable for complexation with  $^{44}\text{Sc}$  at room temperature with appreciable yields for *in vivo* studies. Since the *in vivo* stability of CHX-A''-DTPA complexes is expected to be better than that of conventional



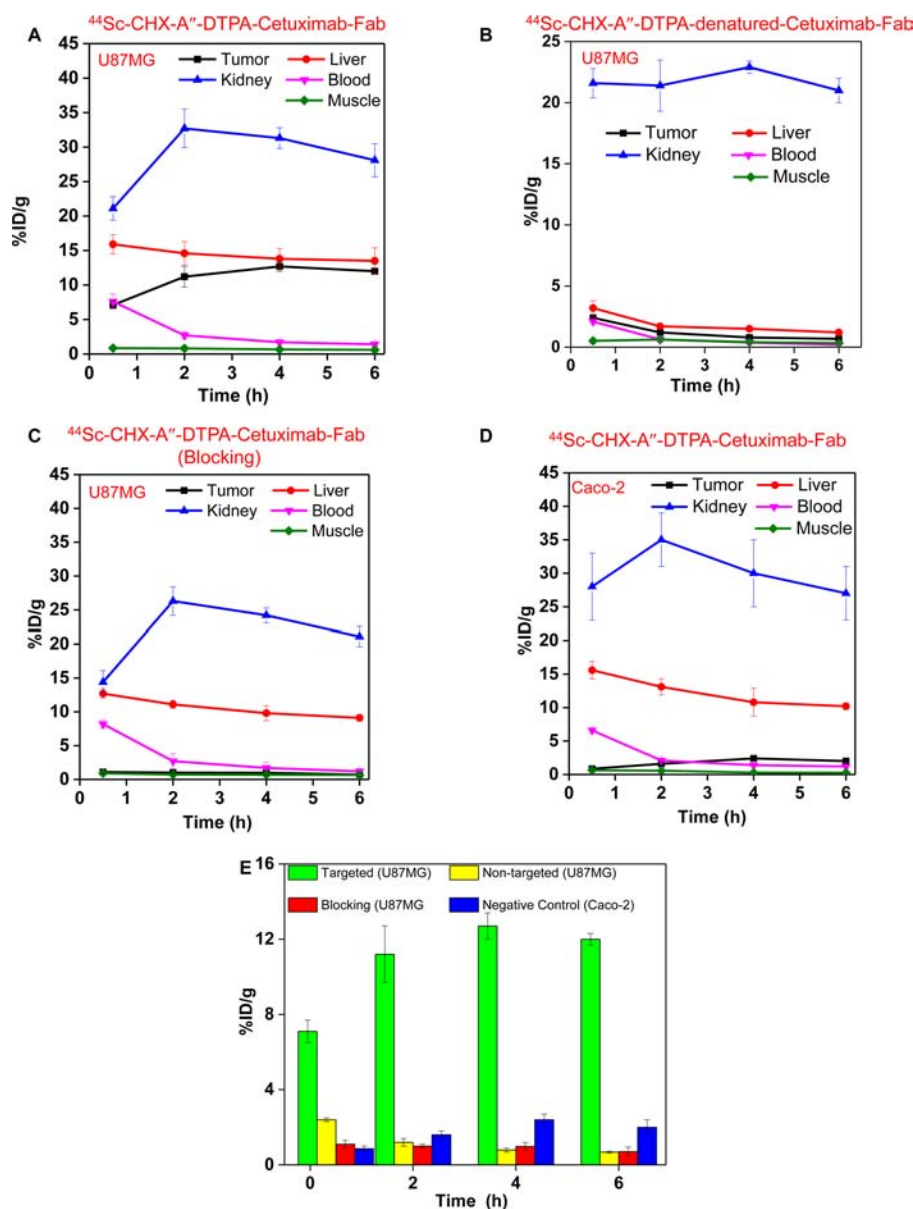


**Figure 4.** Quantitative region-of-interest (ROI) analysis of the PET data. Time–activity curves of the liver, tumor, blood, kidney, and muscle following intravenous injection of (A)  $^{44}\text{Sc}$ -CHX-A''-DTPA-Cetuximab-Fab in U87MG tumor-bearing mice (targeted), (B)  $^{44}\text{Sc}$ -CHX-A''-DTPA-denatured-Cetuximab-Fab in U87MG tumor-bearing mice (non-targeted), (C)  $^{44}\text{Sc}$ -CHX-A''-DTPA-Cetuximab-Fab in U87MG tumor-bearing mice after treatment with a 2 mg blocking dose of Cetuximab (blocking), (D)  $^{44}\text{Sc}$ -CHX-A''-DTPA-Cetuximab-Fab in Caco-2 tumor-bearing mice (negative control). (E) Comparison of tracer uptake in the tumors among all four groups.

DTPA analogues,<sup>20,21</sup>  $^{44}\text{Sc}$ -CHX-A''-DTPA-Cetuximab-Fab was used in all further studies. The specific activity of  $^{44}\text{Sc}$ -CHX-A''-DTPA-Cetuximab-Fab was  $\sim 63 \text{ GBq}/\mu\text{mol}$ , assuming complete recovery of the radiolabeled agent after size-exclusion chromatography. The whole procedure of  $^{44}\text{Sc}$  labeling and purification of the radiolabeled Fab fragment could be completed within 45 min.

Before *in vivo* investigation in mice, serum stability studies were carried out to assess the stability of  $^{44}\text{Sc}$ -CHX-A''-DTPA-Cetuximab-Fab. High serum stability is a prerequisite for *in vivo* applications of a radiolabeled agent. If the radiolabeled complexes are not stable in serum, then  $^{44}\text{Sc}$  may be transchelated by serum proteins, resulting in accumulation of the radioactivity in non-target organs and faulty interpretation of the imaging data obtained. It was found that  $>92\%$  of  $^{44}\text{Sc}$  remained within the CHX-A''-DTPA-

Cetuximab-Fab conjugates over a 6 h incubation period (Figure S3B), indicating high stability of the  $^{44}\text{Sc}$ -CHX-A''-DTPA complex.

**In Vivo PET Imaging and Biodistribution Studies.** The time points of 0.5, 2, 4, and 6 h postinjection (p.i.) were chosen for serial PET scans. The coronal slices that contain the U87MG (high EGFR expression) or Caco-2 (low EGFR expression) tumors are shown in Figure 3A. In addition, representative microPET, microCT, and fused images of a mouse at 4 h p.i. of  $^{44}\text{Sc}$ -CHX-A''-DTPA-Cetuximab-Fab are shown in Figure 3B for direct visual comparison. Quantitative data obtained from ROI analysis of the PET images are shown in Figure 4A–D.  $^{44}\text{Sc}$ -CHX-A''-DTPA-Cetuximab-Fab accumulated rapidly in the tumor and was clearly visible as early as 0.5 h p.i., peaked at 4 h p.i., and remained prominent over time ( $7.1 \pm 0.6$ ,  $11.2 \pm 1.5$ ,  $12.7 \pm 0.7$ , and  $12.0 \pm 0.3\%$  ID/g at 0.5,

2, 4, and 6 h p.i., respectively;  $n = 3$ ; Figures 3A(I) and 4A). The uptake of  $^{44}\text{Sc}$ -CHX-A''-DTPA-Cetuximab-Fab in liver was found to be  $15.9 \pm 1.4$ ,  $14.6 \pm 1.8$ ,  $13.8 \pm 1.6$ , and  $13.5 \pm 1.9\%$  ID/g at 0.5, 2, 4, and 6 h p.i., respectively. Moreover, considerable uptake was observed in the kidneys,  $21.1 \pm 1.7$ ,  $32.7 \pm 2.8$ ,  $31.3 \pm 1.5$ , and  $28.1 \pm 2.4\%$  ID/g at 0.5, 2, 4, and 6 h p.i., respectively ( $n = 3$ ; Figure 4A). This indicates successful clearance of  $^{44}\text{Sc}$ -CHX-A''-DTPA-Cetuximab-Fab fragment through both hepatobiliary and renal pathways, which can be attributed to the much smaller size of the Fab fragment compared to that of the intact Cetuximab antibody (49.9 vs 150 kDa). Radioactivity levels in the blood were found to be  $7.6 \pm 1.1$ ,  $2.7 \pm 0.5$ ,  $1.7 \pm 0.3$ , and  $1.4 \pm 0.2\%$  ID/g at 0.5, 2, 4, and 6 h p.i., respectively ( $n = 3$ ; Figure 4A), indicating significantly faster clearance from the blood than that of radiolabeled intact Cetuximab, which had high ( $\sim 10\%$  ID/g) blood radioactivity levels even at 48 h p.i.<sup>16,22</sup> Furthermore, to confirm that the uptake of the radiolabeled probes was specifically due to EGFR targeting and not a result of the enhanced permeability and retention (EPR) effect in U87MG tumors, serial PET scans with intravenous injections of  $^{44}\text{Sc}$ -CHX-A''-DTPA-denatured-Cetuximab-Fab were also carried out in U87MG tumor-bearing mice ( $n = 3$ ) as a non-targeted control (Figures 3A(II) and 4B).

Administering a blocking dose of Cetuximab significantly reduced the tumor uptake of  $^{44}\text{Sc}$ -CHX-A''-DTPA-Cetuximab-Fab to  $1.1 \pm 0.2$ ,  $0.98 \pm 0.21$ ,  $1.0 \pm 0.1$ , and  $0.71 \pm 0.23\%$  ID/g at 0.5, 2, 4, and 6 h p.i., respectively ( $n = 3$ ; Figures 3A(III) and 4C), further demonstrating the specificity of  $^{44}\text{Sc}$ -CHX-A''-DTPA-Cetuximab-Fab toward EGFR *in vivo*. The specificity of  $^{44}\text{Sc}$ -CHX-A''-DTPA-Cetuximab-Fab was further validated by *in vivo* studies in mice bearing Caco-2 (EGFR negative) tumors, where the tumor uptake was minimal ( $0.86 \pm 0.07$ ,  $1.6 \pm 0.2$ ,  $2.4 \pm 0.3$ , and  $2.0 \pm 0.4\%$  ID/g at 0.5, 2, 4, and 6 h p.i., respectively;  $n = 3$ ), as shown in Figures 3A(IV) and 4D. The radioactivity uptake in all other organs was similar to that of U87MG tumor-bearing mice. Figure 4D summarizes and compares the tumor uptake of  $^{44}\text{Sc}$ -CHX-A''-DTPA-Cetuximab-Fab in all four groups. The differences in tumor % ID/g values were statistically significant ( $P < 0.05$ ;  $n = 3$ ) at all time points examined. After the last PET scans at 6 h p.i., mice were sacrificed, and *ex vivo* biodistribution studies were performed. Good agreement was observed between the biodistribution data and that obtained from ROI quantification of tracer uptake based on PET images at the last time point (Figure 5). The results were further validated by *ex vivo* histological examination (see Supporting Information, Figure S4).

## DISCUSSION

EGFR is a glycosylated transmembrane protein that contributes in several tumorigenic mechanisms including tumor survival, invasion, angiogenesis, and metastatic spread.<sup>11,23</sup> It is also involved in the pathogenesis of many tumors. In many cases, EGFR expression may act as a prognostic indicator, predicting poor survival and/or more advanced disease stages.<sup>9,23</sup> Overexpression of EGFR has been found in several human malignancies such as cancers of the head and neck, esophagus, stomach, pancreas, ovary, cervix, breast, lung, kidney, and bladder.<sup>11</sup> To target EGFR-mediated tumor cell proliferation or growth, a chimeric human–murine IgG1 monoclonal antibody, Cetuximab, has been developed that specifically binds to the EGFR with high affinity.<sup>11</sup> The United States Food and Drug

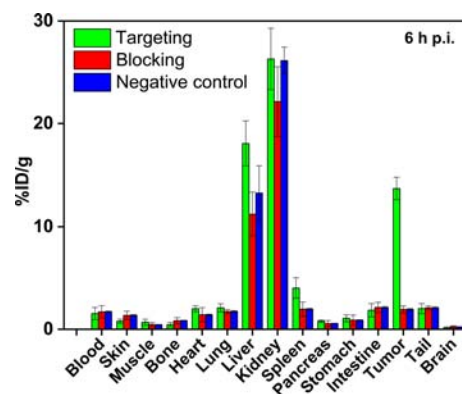


**Figure 5.** Biodistribution of  $^{44}\text{Sc}$ -CHX-A''-DTPA-Cetuximab-Fab in U87MG tumor-bearing mice (targeted),  $^{44}\text{Sc}$ -CHX-A''-DTPA-Cetuximab-Fab in U87MG tumor-bearing mice after treatment with a blocking dose of Cetuximab (blocking), and  $^{44}\text{Sc}$ -CHX-A''-DTPA-Cetuximab-Fab in Caco-2 tumor-bearing mice (negative control) at 6 h p.i. ( $n = 3$ ).

Administration (US FDA) has approved this antibody for treatment of patients with EGFR-expressing metastatic colorectal carcinomas.<sup>11</sup> However, not much is known about patient-specific tumor uptake and the relationship between dosage and efficacy of Cetuximab therapy.<sup>22</sup> Moreover, delayed uptake in tumor and extended circulation times are some major disadvantages associated with the use of intact antibodies for immunoPET studies.<sup>12,14</sup>

Antibody Fab fragments with lower molecular weight compared to that of intact antibodies are expected to display faster blood-/tissue-clearance kinetics, thereby exhibiting a high tumor contrast within 2–3 h after intravenous injection.<sup>12</sup> Moreover, engineered antibody fragments like Fab have been shown to be much less immunogenic than that of intact antibodies, which is further advantageous for molecular imaging.<sup>14</sup> Despite the well-documented use of Cetuximab in molecular imaging and therapy,<sup>10,22,24</sup> there are surprisingly no reports on use of its Fab fragment. The present study showed that  $^{44}\text{Sc}$ -CHX-A''-DTPA-Cetuximab-Fab can be an effective tracer for early noninvasive imaging of EGFR expression in a human glioblastoma (U87MG) tumor model, reported to demonstrate high EGFR expression.<sup>22</sup>  $^{44}\text{Sc}$  was chosen due to its favorable nuclear decay characteristics [ $E_{\beta^+}$  (max) = 1.47 MeV,  $\beta^+$  branching ratio = 94.3%] and its short half-life ( $\sim 3.9$  h), which is very well-suited for imaging applications with antibody fragments with comparable biological half-lives. The high branching ratio of  $^{44}\text{Sc}$  allows a lower amount of activity to be administered for PET imaging, resulting in a lower radiation dose to normal tissues.

There are two main routes for production of  $^{44}\text{Sc}$ . In the first method,  $^{44}\text{Sc}$  can be obtained as a daughter product of  $^{44}\text{Ti}$  via  $^{44}\text{Ti}/^{44}\text{Sc}$  generator.<sup>1</sup> The cyclotron-independent availability of  $^{44}\text{Sc}$  from  $^{44}\text{Ti}/^{44}\text{Sc}$  generator provides the obvious logistic advantages for usage of this excellent radioisotope at remote PET facilities. Owing to the long half-life of  $^{44}\text{Ti}$  ( $t_{1/2} = 59.3$  y), ideally this generator should be able to provide  $^{44}\text{Sc}$  for several decades.<sup>1</sup> However,  $^{44}\text{Ti}$  is produced through the nuclear reaction  $^{45}\text{Sc}(p,2n)^{44}\text{Ti}$ , which requires long-term irradiation of Sc targets at a high proton flux (25 MeV proton, 200  $\mu\text{A}$ ) for production of sufficient quantities of  $^{44}\text{Ti}$ .<sup>3</sup> Presently,  $^{44}\text{Ti}$  can be produced only at a few facilities in the world, with limited yields and at high costs.<sup>1,6</sup> Also,  $^{44}\text{Sc}$  availed from this generator

is not directly amenable for radiopharmaceutical preparation and requires postelution concentration and purification procedures that make the process cumbersome.<sup>25</sup> These undesirable features make the  $^{44}\text{Ti}/^{44}\text{Sc}$  generator impractical for use in clinical context. A more prudent approach is the direct cyclotron production of  $^{44}\text{Sc}$  by proton irradiation of natural calcium targets.<sup>2,6,26,31</sup> There are numerous cyclotron facilities all over the world that can be utilized for cost-effective production of  $^{44}\text{Sc}$  with adequate yields and radionuclidic purity suitable for clinical studies.

A critical component of a  $^{44}\text{Sc}$ -based radiopharmaceuticals is the BFC that binds the radiometal ion in a stable coordination complex and also conjugates with a suitable biomolecule for *in vivo* tumor-targeted imaging.<sup>8,21,27</sup> In order to use  $^{44}\text{Sc}$  for labeling Cetuximab-Fab, it is essential to ensure that the radiolabeling is carried out within a reasonable period of time at room temperature to prevent denaturation of the antibody. Although the thermodynamic stability constant of  $\text{Sc}^{3+}$  complexed with DOTA is much higher than that with other polyaminopolyacetate ligands (Table S1),<sup>27</sup> an adequate radiolabeling yield could not be achieved at room temperature using this BFC. In view of this, use of acyclic DTPA analogues for radiolabeling Cetuximab-Fab appears to be an ideal choice, as they demonstrate rapid complexation kinetics with  $^{44}\text{Sc}^{3+}$  at room temperature. However, DTPA complexes with  $^{90}\text{Y}^{3+}$  (which has similar chemical properties as those of  $^{44}\text{Sc}^{3+}$ , belonging to the same group in the periodic table) have been reported to be kinetically labile when administered *in vivo*.<sup>20,21</sup> The structurally reinforced CHX-A"-DTPA is a significant improvement over the traditional DTPA chelators in terms of increased *in vivo* stability without sacrificing the rapid complexation kinetics.<sup>20,21</sup> This is probably due to the presence of the cyclohexyl group, which increases the rigidity of the structure of the complex, thereby reducing the rate of dissociation.<sup>20</sup> CHX-A"-DTPA-Cetuximab-Fab could be radiolabeled with  $^{44}\text{Sc}$  at room temperature with >60% yield and appreciable specific activity ( $\sim 63 \text{ GBq}/\mu\text{mol}$ ).  $^{44}\text{Sc}$ -CHX-A"-DTPA-Cetuximab-Fab could retain its integrity even when incubated in an excess volume of mouse serum at  $37^\circ\text{C}$  for 6 h, demonstrating its suitability for *in vivo* PET imaging.

*In vivo* PET imaging of EGFR expression in U87MG tumor-bearing mice showed a good uptake of  $^{44}\text{Sc}$ -CHX-A"-DTPA-Cetuximab-Fab as early as 0.5 h after injection of the tracer, with excellent imaging contrast within 2 h. The maximum tumor uptake ( $\sim 12\% \text{ ID/g}$ ) of the radiolabeled Cetuximab-Fab was slightly lower than the maximum tumor uptake ( $\sim 13\% \text{ ID/g}$ ) reported for the intact antibody.<sup>22</sup> This is expected since the Fab fragment lacks the Fc region that has been shown to play an important role in internalization of the antibody.<sup>12,14</sup> However, the lack of Fc reduces nonspecific binding between Fc and its receptors on various types of cells (e.g., macrophages, dendritic cells, neutrophils, natural killer cells, B cells, etc.) and thus improves the tumor-to-normal tissue ratio.<sup>12</sup>

Rapid clearance of  $^{44}\text{Sc}$ -CHX-A"-DTPA-Cetuximab-Fab by renal and hepatobiliary routes enables fast and repeated imaging, which might be helpful in monitoring tumor dynamics. Also, the high tumor-to-blood ratio of  $^{44}\text{Sc}$ -CHX-A"-DTPA-Cetuximab-Fab at early time points would allow same-day PET imaging following radiotracer injection. Thus,  $^{44}\text{Sc}$ -CHX-A"-DTPA-Cetuximab-Fab could overcome the inherent shortcomings of Cetuximab-based immunoPET imaging because of its rapid tumor accumulation and fast background clearance, without significantly compromising

tumor uptake. This strategy can be a valuable asset in selecting patients for anti-EGFR therapy and also for monitoring the therapeutic efficacy of the process.

## CONCLUSIONS

In the present study, we report the successful production and characterization of Cetuximab-Fab. We further demonstrated the feasibility of using cyclotron-produced  $^{44}\text{Sc}$  for radiolabeling the Fab fragments at room temperature in order to image EGFR expression in glioblastoma xenografts in mice. Among the various BFCs studied, CHX-A"-DTPA was identified as the most promising choice as it permits  $^{44}\text{Sc}$  labeling at room temperature within a reasonable period of time.  $^{44}\text{Sc}$ -CHX-A"-DTPA-Cetuximab-Fab could be prepared with high radiolabeling yield and appreciable specific activity suitable for *in vivo* studies. Serum stability studies revealed that the radiolabeled bioconjugate was remarkably stable in mouse serum maintained at  $37^\circ\text{C}$ . Rapid, prominent, and target-specific uptake in U87MG tumors was observed for  $^{44}\text{Sc}$ -CHX-A"-DTPA-Cetuximab-Fab. The radiolabeled agent was rapidly cleared from the biological system by both hepatobiliary and renal routes. This study may further inspire development of new  $^{44}\text{Sc}/^{47}\text{Sc}$ -based radiopharmaceuticals for immunoPET imaging and personalized cancer management.

## EXPERIMENTAL SECTION

**Chemicals.** Erbitux (Cetuximab) was obtained from ImClone LLC, NJ. Fluorescein-labeled secondary antibodies were purchased from Jackson ImmunoResearch Laboratories, Inc. (West Grove, CA). *p*-Isothiocyanato benzyl derivatives of diethylenetriaminepentaacetic acid (*p*-SCN-Bn-DTPA), CHX-A"-DTPA, 1,4,7,10-tetraazacyclododecane-1,4,7,10-tetraacetic acid (*p*-SCN-Bn-DOTA), and 1,4,7-triazacyclononane-1,4,7-triacetic acid (*p*-SCN-Bn-NOTA) were procured from Macrocyclics, Inc. (Dallas, TX). Fluorescein isothiocyanate (FITC) and Chelex-100 resin (50–100 mesh) were purchased from Sigma-Aldrich (St. Louis, MO). AlexaFluor350-NHS ester (NHS denotes *N*-hydroxysuccinimide) was acquired from Invitrogen (Grand Island, NY). PD-10 columns were purchased from GE Healthcare (Piscataway, NJ). Pierce immobilized papain, Pierce Protein A columns, Protein A IgG binding and elution buffers, and all other chemicals were purchased from Thermo Fisher Scientific (Fair Lawn, NJ). Amicon Ultra-15 centrifugal filter units with Ultracel-30 membrane (30K centrifugal filters) of 5 mL capacity were obtained from Millipore (Merck, Germany). Matrigel was purchased from BD Biosciences (Franklin lakes, NJ). Tissue-Tek OCT Compound (embedding medium for frozen tissue specimens) was procured from Sakura (Torrance, CA). Water and all buffers were of Millipore grade and pretreated with Chelex-100 resin to ensure that the aqueous solution was free of heavy metals.

**Generation and Characterization of Cetuximab-Fab.** Cetuximab (2 mg/mL) was digested with immobilized papain (Cetuximab/papain ratio  $\sim 1:40$ ) in a reaction buffer (20 mM sodium phosphate monobasic, 10 mM disodium ethylenediaminetetraacetic acid (EDTA), and 80 mM cysteine-HCl, pH  $\sim 7$ ) for 4 h at  $37^\circ\text{C}$ .<sup>28</sup> Subsequently, the reaction mixture was centrifuged at 5000g for 1 min to remove the immobilized papain. The reaction mixture containing Cetuximab-Fab was subsequently purified by passing through a Protein A column. The concentration of Cetuximab-Fab in the purified solution was determined from UV absorbance at 280



nm using a NanoDrop UV/visible spectrophotometer (Thermo Scientific, USA). The purity of Cetuximab-Fab was evaluated by sodium dodecyl sulfate polyacrylamide gel electrophoresis (SDS-PAGE; 5% stacking gel and 8% resolving gel; non-reducing conditions) using Coomassie brilliant blue R-250 staining. The molecular weight of Cetuximab-Fab was determined by matrix-assisted laser desorption/ionization (MALDI) mass spectrometry, which served as a reference for the Cetuximab-Fab band in SDS-PAGE.

**BFC/FITC/AlexaFluor350 Conjugation of Cetuximab-Fab.** CHX-A"-DTPA conjugation with denatured and intact Cetuximab-Fab was carried out at pH 9.0, maintaining the reaction ratio of CHX-A"-DTPA to Cetuximab-Fab at 10:1. CHX-A"-DTPA–Cetuximab-Fab was purified using PD-10 columns, with PBS as the mobile phase. CHX-A"-DTPA–Cetuximab-Fab eluted between 3.0 and 4.0 mL. The same procedure was adopted for conjugation of other BFCs (*p*-SCN-Bn-DTPA, *p*-SCN-Bn-DOTA, and *p*-SCN-Bn-NOTA). FITC (for flow cytometry analysis) or AlexaFluor350-NHS ester (for histology applications) was also conjugated to Cetuximab-Fab using similar reaction and purification procedures. However, the reaction ratio of FITC or AlexaFluor350-NHS ester to Cetuximab-Fab was 3:1 to limit the number of dyes per Cetuximab-Fab and to avoid self-quenching of the fluorescence signal.

**Flow Cytometry.** The EGFR specificity of Cetuximab-Fab was evaluated by fluorescence-activated cell sorting (FACS) analysis using two cell lines: human glioblastoma cells (U87MG; high EGFR expression<sup>22</sup>) and human epithelial colorectal adenocarcinoma cells (Caco-2; low EGFR expression<sup>29</sup>). Cells were harvested and suspended in cold PBS (pH 7.4) with 2% bovine serum albumin at a concentration of  $5 \times 10^6$  cells/mL and were incubated with FITC–Cetuximab-Fab at 50 nM concentration for 30 min at room temperature, washed, and centrifuged at 1000 rpm for 5 min. Afterward, the cells were analyzed by FACS using a BD FACSCalibur four-color analysis cytometer (Becton-Dickinson, San Jose, CA) and FlowJo analysis software (Tree Star, Inc., Ashland, OR).

**Radiolabeling of Cetuximab-Fab.** Cyclotron-produced  $^{44}\text{Sc}$  (74 MBq)<sup>31</sup> was diluted in 500  $\mu\text{L}$  of 0.5 M sodium acetate buffer (pH 6.5) and added to 40  $\mu\text{g}$  of BFC-conjugated Cetuximab-Fab. The pH of the reaction mixture was carefully adjusted to  $\sim 4.5$ , and the reaction was incubated for 30 min at room temperature (25  $^{\circ}\text{C}$ ) with constant shaking. The radiolabeled agent was purified using PD-10 columns, with PBS as the mobile phase. The radioactive fractions containing  $^{44}\text{Sc}$ -labeled-Cetuximab-Fab (which typically elute between 3 and 4 mL) were collected and used for further *in vivo* PET imaging studies. To determine the radiolabeling yield, the fractions containing Cetuximab-Fab were pooled together, and combined activity was measured and compared with the total activity passed through the column. The radiolabeled agent was passed through a 0.2  $\mu\text{m}$  syringe filter before *in vivo* studies.

**Serum Stability of  $^{44}\text{Sc}$ –CHX-A"-DTPA–Cetuximab-Fab.** In order to determine the *in vitro* stability of  $^{44}\text{Sc}$ –CHX-A"-DTPA–Cetuximab-Fab in mouse serum, 200  $\mu\text{L}$  of the reaction mixture was added to 1.8 mL of mouse serum prewarmed at 37  $^{\circ}\text{C}$  and incubated at the same temperature for different time intervals. As a control, equivalent activity of free  $^{44}\text{ScCl}_3$  (maintained at pH 4.5 in acetate buffer) was incubated with mouse serum under the same conditions. Aliquots were withdrawn at intervals of 15 and 30 min and 1, 2, 4, and 6 h,

and their activities were measured. The aliquot at each time point was taken in a 30 kDa centrifugal filter tube and centrifuged at 5000 rcf for 15 min. The activity of the filtrate was measured, corrected for decay, and compared with the activity of the serum solution (before ultrafiltration) to determine the percentage of free  $^{44}\text{Sc}$  (that detaches from  $^{44}\text{Sc}$ –CHX-A"-DTPA–Cetuximab-Fab) at each time point.

**Animal Models.** All animal studies were conducted under a protocol approved by the University of Wisconsin Institutional Animal Care and Use Committee. U87MG cells and Caco-2 cells were used for tumor inoculation when they reached  $\sim 80\%$  confluence. Four- to five-week-old female athymic nude mice were purchased from Harlan (Indianapolis, IN), and tumors were established by subcutaneously injecting  $5 \times 10^6$  cells, suspended in 100  $\mu\text{L}$  of 1:1 mixture of DMEM medium and matrigel, into the front flank of the mice.<sup>22</sup> The tumor sizes were monitored every alternate day, and *in vivo* experiments were carried out when the diameter of the tumors reached 6–8 mm (typically, 3 weeks after inoculation).

**PET Imaging and Biodistribution Studies.** PET and PET/CT scans at various time points *p.i.*, image reconstruction, and region-of-interest (ROI) analyses were performed using a microPET/microCT Inveon rodent model scanner (Siemens Medical Solutions USA, Inc.) and Inveon Research Workplace [IRW] vendor software, respectively, as described previously.<sup>30</sup> Each tumor-bearing mouse was injected with 1.85–3.7 MBq of  $^{44}\text{Sc}$ –CHX-A"-DTPA–Cetuximab-Fab via the tail vein, and static PET scans were performed. In order to improve the detection statistics and minimize interscan variability due to radioactive decay,  $20 \times 10^6$  coincidence events per mouse were acquired for every static PET emission scan (energy window, 350–650 keV; time window, 3.432 ns; resolution, 1.5 mm). Quantitative data is presented as percentage injected dose per gram (% ID/g) of tissue. Blocking studies were carried out to evaluate EGFR specificity of  $^{44}\text{Sc}$ –CHX-A"-DTPA–Cetuximab-Fab *in vivo*, in which a group of three mice bearing U87MG tumors was injected with 2 mg of Cetuximab 24 h before  $^{44}\text{Sc}$ –CHX-A"-DTPA–Cetuximab-Fab administration. Biodistribution studies were carried out after the last PET scans to validate the PET results. The radioactivity in the tissue was measured using a gamma-counter (PerkinElmer) and presented as percent (%) ID/g.

## ■ ASSOCIATED CONTENT

### ● Supporting Information

$^{44}\text{Sc}$ -labeling yields of Cetuximab-Fab conjugates,  $^{44}\text{Sc}$ -labeling yields under different pH conditions, elution profile of  $^{44}\text{Sc}$ –CHX-A"-DTPA–Cetuximab-Fab from PD-10 column, serum stability of  $^{44}\text{Sc}$ –CHX-A"-DTPA–Cetuximab-Fab, and immunofluorescence staining of tumor and normal tissues. This material is available free of charge via the Internet at <http://pubs.acs.org>.

## ■ AUTHOR INFORMATION

### Corresponding Author

\*E-mail: [wcai@uwhealth.org](mailto:wcai@uwhealth.org); Phone: 608-262-1749; Fax: 608-265-0614.

### Author Contributions

\*R.C. and S.G. contributed equally to this work.

### Notes

The authors declare no competing financial interest.

## ■ ACKNOWLEDGMENTS

This work is supported, in part, by the University of Wisconsin–Madison, the National Institutes of Health (NIBIB/NCI 1R01CA169365 and P30CA014520), the Department of Defense (W81XWH-11-1-0644), the American Cancer Society (125246-RSG-13-099-01-CCE), US Department of Energy (DOE-SC0008384), and the Fulbright Scholar Program (1831/FNPDR/2013).

## ■ REFERENCES

- (1) Roesch, F. (2012) Scandium-44: benefits of a long-lived PET radionuclide available from the  $^{44}\text{Ti}/^{44}\text{Sc}$  generator system. *Curr. Radiopharm.* 5, 187–201.
- (2) Severin, G. W., Engle, J. W., Valdovinos, H. F., Barnhart, T. E., and Nickles, R. J. (2012) Cyclotron produced  $^{44}\text{Sc}$  from natural calcium. *Appl. Radiat. Isot.* 70, 1526–30.
- (3) Cutler, C. S., Hennkens, H. M., Sisay, N., Huclier-Markai, S., and Jurisson, S. S. (2013) Radiometals for combined imaging and therapy. *Chem. Rev.* 113, 858–83.
- (4) Koumariannou, E., Loktionova, N. S., Fellner, M., Roesch, F., Thews, O., Pawlak, D., Archimandritis, S. C., and Mikolajczak, R. (2012)  $^{44}\text{Sc}$ -DOTA-BN[2–14] $\text{NH}_2$  in comparison to  $^{68}\text{Ga}$ -DOTA-BN[2–14] $\text{NH}_2$  in pre-clinical investigation. Is  $^{44}\text{Sc}$  a potential radionuclide for PET? *Appl. Radiat. Isot.* 70, 2669–76.
- (5) Eigner, S., Vera, D. R., Fellner, M., Loktionova, N. S., Piel, M., Lebeda, O., Rosch, F., Ross, T. L., and Henke, K. E. (2013) Imaging of protein synthesis: in vitro and in vivo evaluation of  $^{44}\text{Sc}$ -DOTA-puromycin. *Mol. Imaging Biol.* 15, 79–86.
- (6) Muller, C., Bunka, M., Reber, J., Fischer, C., Zhernosekov, K., Turler, A., and Schibli, R. (2013) Promises of cyclotron-produced  $^{44}\text{Sc}$  as a diagnostic match for trivalent beta-emitters: in vitro and in vivo study of a  $^{44}\text{Sc}$ -DOTA-folate conjugate. *J. Nucl. Med.* 54, 2168–74.
- (7) Hernandez, R., Valdovinos, H. F., Yang, Y., Chakravarty, R., Hong, H., Barnhart, T. E., and Cai, W. (2014)  $^{44}\text{Sc}$ : an attractive isotope for peptide-based PET imaging. *Mol. Pharmaceutics* 11, 2954–61.
- (8) Majkowska-Pilip, A., and Bilewicz, A. (2011) Macrocyclic complexes of scandium radionuclides as precursors for diagnostic and therapeutic radiopharmaceuticals. *J. Inorg. Biochem* 105, 313–20.
- (9) Corcoran, E. B., and Hanson, R. N. (2014) Imaging EGFR and HER2 by PET and SPECT: a review. *Med. Res. Rev.* 34, 596–643.
- (10) Harding, J., and Burtneiss, B. (2005) Cetuximab: an epidermal growth factor receptor chimeric human-murine monoclonal antibody. *Drugs Today* 41, 107–27.
- (11) Sihver, W., Pietzsch, J., Krause, M., Baumann, M., Steinbach, J., and Pietzsch, H. J. (2014) Radiolabeled cetuximab conjugates for EGFR targeted cancer diagnostics and therapy. *Pharmaceutics* 7, 311–38.
- (12) Olafsen, T., and Wu, A. M. (2010) Antibody vectors for imaging. *Semin. Nucl. Med.* 40, 167–81.
- (13) Romer, T., Leonhardt, H., and Rothbauer, U. (2011) Engineering antibodies and proteins for molecular in vivo imaging. *Curr. Opin. Biotechnol.* 22, 882–7.
- (14) Holliger, P., and Hudson, P. J. (2005) Engineered antibody fragments and the rise of single domains. *Nat. Biotechnol.* 23, 1126–36.
- (15) van Dijk, L. K., Hoeben, B. A., Stegeman, H., Kaanders, J. H., Franssen, G. M., Boerman, O. C., and Bussink, J. (2013)  $^{111}\text{In}$ -cetuximab-F(ab')<sub>2</sub> SPECT imaging for quantification of accessible epidermal growth factor receptors (EGFR) in HNSCC xenografts. *Radiother. Oncol.* 108, 484–8.
- (16) van Dijk, L. K., Hoeben, B. A., Kaanders, J. H., Franssen, G. M., Boerman, O. C., and Bussink, J. (2013) Imaging of epidermal growth factor receptor expression in head and neck cancer with SPECT/CT and  $^{111}\text{In}$ -labeled cetuximab-F(ab')<sub>2</sub>. *J. Nucl. Med.* 54, 2118–24.
- (17) Bork, C., Holdridge, S., Walter, M., Fallon, E., and Pohlschmidt, M. (2014) Online integrity monitoring in the protein A step of mAb production processes-increasing reliability and process robustness. *Biotechnol. Prog.* 30, 383–90.
- (18) Shamashkin, M., Godavarti, R., Iskra, T., and Coffman, J. (2013) A tandem laboratory scale protein purification process using Protein A affinity and anion exchange chromatography operated in a weak partitioning mode. *Biotechnol. Bioeng.* 110, 2655–63.
- (19) Wang, L., Dembecki, J., Jaffe, N. E., O'Mara, B. W., Cai, H., Sparks, C. N., Zhang, J., Laino, S. G., Russell, R. J., and Wang, M. (2013) A safe, effective, and facility compatible cleaning in place procedure for affinity resin in large-scale monoclonal antibody purification. *J. Chromatogr. A* 1308, 86–95.
- (20) Chakravarty, R., Chakraborty, S., and Dash, A. (2014) A systematic comparative evaluation of  $^{90}\text{Y}$ -labeled bifunctional chelators for their use in targeted therapy. *J. Labelled Compd. Radiopharm.* 57, 65–74.
- (21) Brechbiel, M. W. (2008) Bifunctional chelates for metal nuclides. *Q. J. Nucl. Med. Mol. Imaging* 52, 166–73.
- (22) Cai, W., Chen, K., He, L., Cao, Q., Koong, A., and Chen, X. (2007) Quantitative PET of EGFR expression in xenograft-bearing mice using  $^{64}\text{Cu}$ -labeled cetuximab, a chimeric anti-EGFR monoclonal antibody. *Eur. J. Nucl. Med. Mol. Imaging* 34, 850–8.
- (23) Herbst, R. S. (2004) Review of epidermal growth factor receptor biology. *Int. J. Radiat. Oncol. Biol. Phys.* 59, 21–6.
- (24) Aerts, H. J., Dubois, L., Perk, L., Vermaelen, P., van Dongen, G. A., Wouters, B. G., and Lambin, P. (2009) Disparity between in vivo EGFR expression and  $^{89}\text{Zr}$ -labeled cetuximab uptake assessed with PET. *J. Nucl. Med.* 50, 123–31.
- (25) Pruszyński, M., Loktionova, N. S., Filosofov, D. V., and Rosch, F. (2010) Post-elution processing of  $^{44}\text{Ti}/^{44}\text{Sc}$  generator-derived  $^{44}\text{Sc}$  for clinical application. *Appl. Radiat. Isot.* 68, 1636–41.
- (26) Hoehr, C., Oehlke, E., Benard, F., Lee, C. J., Hou, X., Badesso, B., Ferguson, S., Miao, Q., Yang, H., Buckley, K., Hanemaayer, V., Zeisler, S., Ruth, T., Celler, A., and Schaffer, P. (2014)  $^{44}\text{Sc}$  production using a water target on a 13 MeV cyclotron. *Nucl. Med. Biol.* 41, 401–6.
- (27) Price, E. W., and Orvig, C. (2014) Matching chelators to radiometals for radiopharmaceuticals. *Chem. Soc. Rev.* 43, 260–90.
- (28) Andrew, S. M., Pimm, M. V., Perkins, A. C., and Baldwin, R. W. (1986) Comparative imaging and biodistribution studies with an anti-CEA monoclonal antibody and its F(ab)<sub>2</sub> and Fab fragments in mice with colon carcinoma xenografts. *Eur. J. Nucl. Med.* 12, 168–75.
- (29) Xu, H., Yu, Y., Marciniak, D., Rishi, A. K., Sarkar, F. H., Kucuk, O., and Majumdar, A. P. (2005) Epidermal growth factor receptor (EGFR)-related protein inhibits multiple members of the EGFR family in colon and breast cancer cells. *Mol. Cancer Ther.* 4, 435–42.
- (30) Zhang, Y., Hong, H., Orbay, H., Valdovinos, H. F., Nayak, T. R., Theuer, C. P., Barnhart, T. E., and Cai, W. (2013) PET imaging of CD105/endoglin expression with a  $^{61}/^{64}\text{Cu}$ -labeled Fab antibody fragment. *Eur. J. Nucl. Med. Mol. Imaging* 40, 759–67.
- (31) Valdovinos, H. F., Hernandez, R., Barnhart, T. E., Graves, S., and Nickles, R. J. (2014) Separation of cyclotron-produced  $^{44}\text{Sc}$  from a natural calcium target using a dipentyl pentylphosphonate functionalized extraction resin. *Appl. Radiat. Isot.* 95, 23–9.